Dynamic Stability of a Sandwich Beam with an Electrorheological Fluid Core

S.C.Mohanty
Department of Mechanical Engineering,
National Institute of Technology, Rourkela,
Pin-769008, ORISSA, INDIA.
Email: scmohanty@nitrkl.ac.in

ABSTRACT

In the present study the parametric instability of a three layer sandwich beam with an embedded thick electrorheological(ER) fluid core has been studied. The beam has been modeled using finite elements and the regions of instability have been established using Saito and Otomi conditions. The ER core model is based on the pre-yield rheological properties and is represented by the complex modulus. The sandwich model takes in to account the shear, transverse and longitudinal deformations of the viscoelastic core. The effects of electric field strength and core thickness parameter on the fundamental frequency, fundamental buckling load and fundamental system loss factor have been studied. The effects of parameters like electric field and thickness parameter on the stability behavior of the beam have been investigated. The increase in electric field strength and core thickness has stabilizing effect for all the boundary conditions.

1. INTRODUCTION

Electrorheological (ER) fluids transform to solid like gel upon application of an electric field. The stiffness and damping depend on the magnitude of the applied voltage. Winslow first discovered electrorheological fluid (ER) in the year 1949[1]. Block et al. reported that the change in material properties is reversible and occurs in milliseconds[2]. Coulter reported the use of this innovative fluid in numerous engineering applications, including antivibration mounts, clutches, and dampers [3]. Weiss et al. presented a summary of the state of research and development of electrorheological fluid [4]. The earliest work on sandwich construction incorporating ER fluids is that of Gandhi et al., wherein it is shown that substantial improvements in stiffness and damping can be achieved using ER fluids[5].The concept of electrorheological material-based adaptive structures was introduced in a patent issued by Carlson et al.[6]. Yalcintas and Coulter developed a theoretical model based on Mead and Markus (MM) model for adaptive beam structures with various boundary conditions[7]. Yalcintas and Coulter extended the Ross, Kerwin and Ungar (RKU) model to investigate the forced flexural vibration of simply supported laminated adaptive beams having ER material as a controllable damping layer [8]. Don and Coulter carried out an indepth theoretical and experimental investigation to study the utility of RKU and MM models, in predicting the dynamic behavior of ER based structures[9]. Yalcintas and Dai analyzed the vibration control capabilities of adaptive structures made of electrorheological and magnetorheological materials, and compared their vibration minimization rates, time responses, and energy consumption rates[10]. Lee presented a linear finite element model for a sandwich beam with embedded electrorheological fluids using linearized complex moduli of the fluid[11]. Rezaeepazhand and Pahlavan studied the transient response of a three layer sandwich beam with an electrorheological fluid core[12]. They modeled the core as Bingham plastic model.

Many investigators have studied the dynamic stability of beams applying finite element method. Brown et al. studied the dynamic stability of uniform bars by applying this method[13]. Abbas studied the effect of rotational speed and root flexibility on the stability of a rotating Timoshenko beam by finite element method[14]. Abbas and Thomas and Yokoyama used finite element method to study the effect of support condition on the dynamic stability of Timoshenko beams[15,16]. Briseghella et al. studied the dynamic stability problems of beams and

frames by using finite element method [17]. Svensson by this method studied the stability properties of a periodically loaded non-linear dynamic system, giving special attention to damping effects [18]. Mohanty used finite element method along with Saito Otomi criteria to establish the stability boundaries for multilayered cantilever symmetric sandwich beam with viscoelastic core [19]. Yeh et al. studied the dynamic stability of a sandwich beam with a constrained layer and electrorheological fluid core using harmonic balance method [20]. Mohanty investigated the parametric instability of a pretwisted cantilever beam with localised damage[21]. He established the instability regions applying Floquet's theory.

In the present study the parametric instability of a three layer cantilever sandwich beam with an electrorheological fluid core has been studied. The beam is modeled using finite element and the regions of instability are established using Saito and Otomi[22] conditions. The ER core model is based on the pre-yield rheological properties and is represented by the complex Young's and Shear modulus. The sandwich model takes in to account the shear, traverse and longitudinal deformation of the soft ER core. The effects of electric field and thickness parameter on the stability of the beam have been investigated.

2. FORMULATION OF THE PROBLEM

Figure (1) shows a three layered symmetric sandwich beam of length L and width b respectively, subjected to a pulsating axial force $P(t)= P_s+P_d \cos\Omega t$ acting along its undeformed axis at one end. P_s is the static and P_d is the amplitude of the time dependent dynamic component of the load acting along its undeformed axis at the free end and Ω is the excitation frequency of the dynamic load component.
The finite element model is developed based on the following assumptions:
(1) The rotary inertia and shear deformations in the constraining layers are negligible.
(2) Linear theories of elasticity and viscoelasticity are used.
(3) No slip occurs between the layers and there is perfect continuity at the interfaces.

2.1 Element matrices

As shown in figure (2) the element model presented here consists of two nodes and each node has six degrees of freedom. Nodal displacements are given by

$$\{\Delta^e\} =\{u_{1i}\ \ u_{3i}\ \ w_{1i}\ w_{3i}\ \theta_{1i}\ \theta_{3i}\ u_{1j}\ u_{3j}\ w_{1j}\ w_{3j}\ \theta_{1j}\ \theta_{3j}\}^T \quad (1)$$

where i and j are elemental nodal numbers. The axial displacement of the constraining layer, the transverse displacement and the rotational angle, can be expressed in terms of nodal displacements and finite element shape functions.

$$u_1 = [\,Nu_1\,]\,\{\Delta^e\},\ u_3 = [\,Nu_3\,]\,\{\Delta^e\},\ w_1 = [\,N_{w1}\,]\,\{\Delta^e\},\ w_3 = [\,N_{w3}\,]\,\{\Delta^e\},$$
$$\theta_1= [N_w]'\{\Delta^e\},\ \theta_3= [N_{w3}]'\{\Delta^e\} \quad (2)$$

where the prime denotes differentiation with respect to axial coordinate x and the shape functions are given by

$$[\,Nu_1\,] = [1-\xi\ 0\ 0\ 0\ 0\ 0\ \xi\ 0\ 0\ 0\ 0\ 0]$$
$$[\,Nu_3\,] = [0\ 1-\xi\ 0\ 0\ 0\ 0\ 0\ \xi\ 0\ 0\ 0\ 0]$$
$$[\,N_{w1}\,] = [\,0\ \ 0\ \ (1-3\xi^2+2\xi^3)\ \ 0\ (\xi-2\xi^2+\xi^3)L_e\ \ 0\ \ 0\ \ 0\ 3\xi^2-2\xi^3\ \ 0\ (-\xi^2+\xi^3)\,L_e\ \ 0\,]$$
$$[\,N_{w3}\,] = [\,0\ \ 0\ \ 0\ (1-3\xi^2+2\xi^3)\ \ 0\ (\xi-2\xi^2+\xi^3)L_e\ \ 0\ \ 0\ \ 0\ 3\xi^2-2\xi^3\ \ 0\ \ (-\xi^2+\xi^3)\,L_e\,]$$

where $\xi = x / L_e$ *and* L_e is the length of the element.

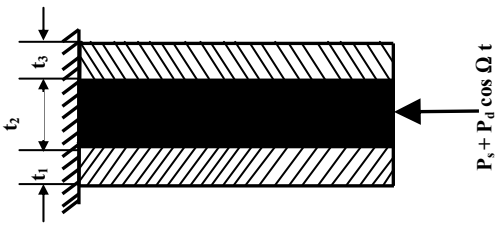

Figure (1) Cantilever Sandwich Beam with ER fluid Core

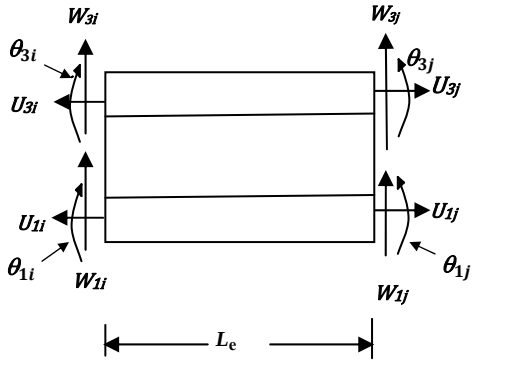

Fig.2 Finite Beam Element for a Layered Sandwich Beam

2.1.1 Element stiffness matrix, $\left[K^{(e)}\right]$

Elemental potential energy ($U^{(e)}$) is equal to the sum of the potential energy of the constraining layers and viscoelastic layers.

$$U^{(e)} = U_c^{(e)} + U_v^{(e)} \tag{3}$$

The potential energy of the constraining layers due to bending and axial extension is given as

$$U_c^{(e)} = \sum_{k=1,2} \frac{1}{2} \int_0^l E_{(2k-1)}\, I_{(2k-1)} \left(\frac{\partial^2 w_{(2k-1)}}{\partial x^2} \right)^2 dx + \sum_{k=1,2} \frac{1}{2} \int_0^l E_{(2k-1)}\, A_{(2k-1)} \left(\frac{\partial u_{(2k-1)}}{\partial x} \right)^2 dx \tag{4}$$

where $E_{(2k-1)}$, $A_{(2k-1)} = b\{t_{(2k-1)}\}$ and $I_{(2k-1)} = b\{t_{(2k-1)}\}^3/12$ are the Young's modulus, cross-sectional area and area moment of inertia of the (*2k-1*)th constraining layer respectively.

By substituting eq.(2) in to eq. (4) the element potential energy of the constraining layers can be written as

$$U_c^{(e)} = \sum_{k=1}^{n+1} \frac{1}{2} \{\Delta^{(e)}\}^T \left(\left[K^{(e)}_{(2k-1)w}\right] + \left[K^{(e)}_{(2k-1)u}\right] \right) \{\Delta^{(e)}\} \tag{5}$$

$$\left.\begin{aligned} \left[K^{(e)}_{(2k-1)u}\right] &= E_{(2k-1)}\, A_{(2k-1)} \int_0^l \left[N_{(2k-1)}\right]^T \left[N_{(2k-1)}\right]' \, dx \\ \left[K^{(e)}_{(2k-1)w}\right] &= E_{(2k-1)}\, I_{(2k-1)} \int_0^l \left[N_w\right]''^T \left[N_w\right]'' \, dx \end{aligned}\right\} \tag{6}$$

The potential energy of the viscoelastic layers due to shear, longitudinal and transverse deformations is given as

$$U_v^{(e)} = \frac{1}{2}\int_0^l G_v A_v \gamma_v^2 dx + \frac{1}{2}\int_0^l E_v A_v \varepsilon_{vL}^2 dx + \frac{1}{2}\int_0^l E_v A_v \varepsilon_{vT}^2 dx \tag{7}$$

where A_v is the cross-sectional area and G_v is the complex shear modulus of viscoelastic layer. E_v is the complex Young's modulus of viscoelastic layer.

The shear strain γ_v, longitudinal strain (ε_{vL}) and transverse shear strain (ε_{vT}) due to thickness deformation of the viscoelastic layer from kinematic relationship between the constraining layers is expressed as follows:

$$\left.\begin{aligned} \gamma_v &= \frac{u_1 - u_3}{2} + \frac{(t_1+t_2)}{2t_2}\frac{\partial w_1}{\partial x} + \frac{(t_2+t_3)}{2t_2}\frac{\partial w_3}{\partial x} \\ \varepsilon_{vL} &= \frac{1}{2}\left(\frac{\partial u_1}{\partial x} + \frac{\partial u_3}{\partial x}\right) + \frac{t_1}{4}\left(\frac{\partial w_1}{\partial x}\right) - \frac{t_3}{4}\left(\frac{\partial w_3}{\partial x}\right) \\ \varepsilon_{vT} &= \left(\frac{w_1 - w_3}{t_2}\right) \end{aligned}\right\} \tag{8}$$

Substituting Eq. (2) in to Eq. (8) $\gamma_v, \varepsilon_{vL}, \varepsilon_{vT}$ and $u_v$can be expressed in terms of nodal displacements and element shape functions:

$$\left.\begin{aligned} \gamma_{\mathrm{v}} &= \left[N_\gamma\right]\{\Delta^{(e)}\} \\ \varepsilon_{\mathrm{vL}} &= [N_L]\{\Delta^{(e)}\} \\ \varepsilon_{\mathrm{vT}} &= [N_T]\{\Delta^{(e)}\} \end{aligned}\right\} \tag{9}$$

Where,

$$\left.\begin{aligned} \left[N_\gamma\right] &= \frac{([N_{u1}] - [N_{u1}])}{t_2} + \frac{(t_1+t_2)}{2t_2}[N_{w1}] - \frac{(t_3+t_2)}{2t_2}[N_{w3}] \\ [N_L] &= \frac{1}{2}([N_{u1}]' + [N_{u3}]') + \frac{t_1}{4}[N_{w1}]'' - \frac{t_3}{4}[N_{w3}]'' \\ [N_T] &= \frac{1}{t_2}([N_{w1}] - [N_{w3}]) \end{aligned}\right\} \tag{10}$$

Substituting eq. (9) in to eq. (7) the potential energy of the viscoelastic material layer is given by

$$U_v^{(e)} = \frac{1}{2}\{\Delta^{(e)}\}^T \left(\left[K_{v\gamma}^{(e)}\right] + \left[K_{vL}^{(e)}\right] + \left[K_{vT}^{(e)}\right] \right) \{\Delta^{(e)}\} \tag{11}$$

$$\left.\begin{aligned}\left[K_{v\gamma}^{(e)}\right] &= G_v A_v \int_0^l [N_\gamma]^T [N_\gamma] dx \\ \left[K_{vL}^{(e)}\right] &= E_v A_v \int_0^l [N_L]^T [N_L] dx \\ \left[K_{vT}^{(e)}\right] &= E_v A_v \int_0^l [N_T]^T [N_T] dx\end{aligned}\right\} \quad (12)$$

Potential energy of the element

$$U^{(e)} = \sum_{k=1,2} \frac{1}{2}\{\Delta^{(e)}\}^T \left(\left[K_{(2k-1)u}^{(e)}\right] + \left[K_{(2k-1)w}^{(e)}\right]\right)\{\Delta^{(e)}\} + \frac{1}{2}\{\Delta^{(e)}\}^T \left(\left[K_{v\gamma}^{(e)}\right] + \left[K_{vL}^{(e)}\right] + \left[K_{vT}^{(e)}\right]\right)\{\Delta^{(e)}\} \quad (13)$$

$$U^{(e)} = \frac{1}{2}\{\Delta^{(e)}\}^T [K^{(e)}]\{\Delta^{(e)}\} \quad (14)$$

$$[K^{(e)}] = \sum_{k=1,2} \left(\left[K_{(2k-1)u}^{(e)}\right] + \left[K_{(2k-1)w}^{(e)}\right]\right) + \left[K_{v\gamma}^{(e)}\right] + \left[K_{vL}^{(e)}\right] + \left[K_{vT}^{(e)}\right] \quad (15)$$

$[K^{(e)}]$ is the element stiffness matrix.

2.1.2 Element Mass Matrix, $[M^{(e)}]$

Elemental kinetic energy ($T^{(e)}$) is equal to the sum of the kinetic energy of the constraining layers and viscoelastic layers.

$$T^{(e)} = T_c^{(e)} + T_v^{(e)} \quad (16)$$

$$T_c^{(e)} = \sum_{k=1,2} \frac{1}{2}\int_0^l \rho_{(2k-1)} A_{(2k-1)} \left(\frac{\partial w_{(2k-1)}}{\partial t}\right)^2 dx + \frac{1}{2}\int_0^l \rho_{(2k-1)} A_{(2k-1)} \left(\frac{\partial u_{(2k-1)}}{\partial t}\right)^2 dx \quad (17)$$

where $\rho_{(2k-1)}$ is the mass density of the (*2k-1*)th constraining layer.

By substituting eq. (2) in to eq. (17), the element kinetic energy of the constraining layers can be written as

$$T_c^{(e)} = \sum_{k=1,2} \frac{1}{2} \{\dot{\Delta}^{(e)}\}^T \left(\left[M_{(2k-1)u}^{(e)}\right] + \left[M_{(2k-1)w}^{(e)}\right]\right) \{\dot{\Delta}^{(e)}\} \quad (18)$$

$$\left[M_{(2k-1)u}^{(e)}\right] = \rho_{(2k-1)} A_{(2k-1)} \int_0^l \left[N_{(2k-1)u}\right]^T \left[N_{(2k-1)u}\right] dx \quad (19)$$

$$\left[M_{(2k-1)w}^{(e)}\right] = \rho_{(2k-1)} A_{(2k-1)} \int_0^l \left[N_{(2k-1)w}\right]^T \left[N_{(2k-1)w}\right] dx \quad (20)$$

Kinetic energy of the viscoelastic layers is written as

$$T_v^{(e)} = \frac{1}{2}\int_0^l \rho_v A_v \left\{\left(\frac{\partial w_v}{\partial t}\right)^2 + \left(\frac{\partial u_v}{\partial t}\right)^2\right\} dx \quad (21)$$

where A_v is the cross-sectional area and ρ_v is the mass density of the viscoelastic layer

$$u_v = \frac{u_3 + u_1}{2} + \frac{t_1}{4}\frac{\partial w_1}{\partial x} - \frac{t_3}{4}\frac{\partial w_3}{\partial x} \quad (22)$$

$$w_v = \frac{w_3 + w_1}{2} \quad (23)$$

Substituting eq. (2) in to eq. (22) and eq.(23), u_v and w_v can be expressed in terms of nodal displacements and element shape functions:

$$\left.\begin{aligned}u_v &= [N_{vL}]\{\Delta^{(e)}\} \\ w_v &= [N_{vT}]\{\Delta^{(e)}\}\end{aligned}\right\} \quad (24)$$

Where,

$$\left.\begin{aligned}[N_{vL}] &= \frac{1}{2}([N_{u3}] + [N_{u1}]) + \frac{t_1}{4}[N_{w1}] - \frac{t_3}{4}[N_{w3}] \\ [N_{vT}] &= \frac{1}{2}([N_{w3}] + [N_{w1}])\end{aligned}\right\} \quad (25)$$

Substituting eq. (24) in to eq. (21) , the kinetic energy of viscoelastic material layers is given by

$$T_v^{(e)} = \frac{1}{2}\{\dot{\Delta}^{(e)}\}^T \left(\left[M_{vL}^{(e)}\right] + \left[M_{vT}^{(e)}\right]\right)\{\dot{\Delta}^{(e)}\} \quad (26)$$

where,

$$\left.\begin{aligned}\left[M_{vL}^{(e)}\right] &= \rho_v A_v \int_0^l [N_{vL}]^T [N_{vL}] dx \\ \left[M_{vT}^{(e)}\right] &= \rho_v A_v \int_0^l [N_{vT}]^T [N_{vT}] dx\end{aligned}\right\} \quad (27)$$

$$T^{(e)} = T_c^{(e)} + T_v^{(e)} =$$

$$\sum_{k=1,2} \frac{1}{2}\{\dot{\Delta}^{(e)}\}^T \left(\left[M_{(2k-1)u}^{(e)}\right] + \left[M_{(2k-1)w}^{(e)}\right]\right)\{\dot{\Delta}^{(e)}\} + \frac{1}{2}\{\dot{\Delta}^{(e)}\}^T \left(\left[M_{vL}^{(e)}\right] + \left[M_{vT}^{(e)}\right]\right)\{\dot{\Delta}^{(e)}\}$$

$$T^{(e)} = \frac{1}{2}\{\dot{\Delta}^{(e)}\}^T [M^{(e)}]\{\dot{\Delta}^{(e)}\} \quad (28)$$

$$[M^{(e)}] = \sum_{k=1,2} \left(\left[M_{(2k-1)u}^{(e)}\right] + \left[M_{(2k-1)w}^{(e)}\right]\right) + \left(\left[M_{vL}^{(e)}\right] + \left[M_{vT}^{(e)}\right]\right) \quad (29)$$

2.1.3 Element Geometric Stiffness Matrix, $[K_g^{(e)}]$

The elemental work done by axial periodic force $P(t)$ is written as

$$W_p^{(e)} = \frac{1}{2} \sum_{k=1,2} \int_0^l P(t) \left(\frac{\partial w_{(2k-1)}}{\partial x}\right)^2 dx = \frac{1}{2} \{\Delta^{(e)}\}^T P(t) K_g^{(e)} \{\Delta^{(e)}\} \quad (30)$$

where $[K_g^{(e)}] = \sum_{k=1,2} \int_0^l \left[N_{w(2k-1)}\right]^T \left[N_{w(2k-1)}\right] dx$, the elemental geometric stiffness matrix.

2.2 Governing equations of motions

The equation of motion for the beam is written as

$$[M]\{\ddot{\Delta}\} + [K]\{\Delta\} - P(t)[K_g]\{\Delta\} = 0 \quad (31)$$

where $\{\Delta\}$ is the global displacement matrix.

Let $P_s = \alpha P^*$ and $P_t = \beta P^*$ and, where $P^* = D/L^2$ and $D = \sum_{k=1}^{n+1} E_{(2k-1)} I_{(2k-1)}$. Hence $P(t) = \alpha P^* + \beta P^* \cos \Omega t$, where α and β are static and dynamic load factors respectively,equation(20) becomes

$$[M]\{\ddot{\Delta}\} + \left([K] - P_s [K_g]_s\right)\{\Delta\} - P_t \cos \Omega t [K_g]_t \{\Delta\} = 0 \quad (32)$$

where the matrices $[K_g]_s$ and $[K_g]_t$ reflect the influence of P_s and P_t respectively. If the static and time dependent component of loads are applied in the same manner, then

$[K_g]_s = [K_g]_t = [K_g]$.

$$[M]\{\ddot{\Delta}\} + [\overline{K}]\{\Delta\} - (\beta P^* \cos \Omega t)[K_g]\{\Delta\} = 0 \quad (33)$$

The global displacement matrix $\{\Delta\}$ can be assumed as

$$\{\Delta\} = [\Phi]\{\Gamma\} \quad (34)$$

where $[\Phi]$ is the normalized modal matrix corresponding to

$$[M]\{\ddot{\Delta}\} + [\overline{K}]\{\Delta\} = 0 \quad (35)$$

and $\{\Gamma\}$ is a new set of generalised coordinates .

Substituting equation(23) in equation(22), equation(22) is transformed to the following set of N_c coupled Mathieu equations.

$$\ddot{\Gamma}_m + (\omega_m^2)\Gamma_m + \beta P^* \cos \Omega t \sum_{n=1}^{N_c} b_{mn} \Gamma_n = 0 \qquad m = 1,2,..... N_c. \quad (36)$$

where (ω_m^2) are the distinct eigenvalues of $[M]^{-1}[\overline{K}]$ and b_{mn} are the elements of the complex matrix $[B] = -[\Phi]^{-1}[M]^{-1}[K_g][\Phi]$ and $\omega_m = \omega_{m.R} + i\,\omega_{m.I}$, $b_{mn} = b_{mn.R} + i\,b_{mn.I}$ and $i = \sqrt{-1}$

2.3 Regions of Instability

The boundaries of the regions of instability for simple and combination resonance are obtained by applying the following conditions [1] to the Equation 36.

Case (A): Simple resonance

The boundaries of the instability regions are given by

$$\left|\frac{\Omega}{2\omega_0}-\overline{\omega}_{\mu,R}\right|<\frac{1}{4}\left[\frac{\beta^2(b^2{}_{\mu\mu,R}+b^2{}_{\mu\mu,I})}{\overline{\omega}^2{}_{\mu,R}}-16\,\overline{\omega}^{-2}{}_{\mu,I}\right]^{1/2},\quad \mu=1,2\ldots\ldots N_c. \tag{37}$$

where $\omega_0=\sqrt{D/mL^4}$, $\overline{\omega}_{\mu,R}=\omega_{\mu,R}/\omega_0$, $\overline{\omega}_{\mu,I}=\omega_{\mu,I}/\omega_0$, m is mass per unit length of the sandwich beam.

Case (B): Combination resonance of sum type

The boundaries of the regions of instability of sum type are given by

$$\left|\frac{\Omega}{2\omega_0}-\frac{1}{2}(\overline{\omega}_{\mu,R}+\overline{\omega}_{\nu,R})\right|<\frac{1}{8}\frac{(\overline{\omega}_{\mu,I}+\overline{\omega}_{\nu,I})}{(\overline{\omega}_{\mu,I}\,\overline{\omega}_{\nu,I})^{1/2}}\left[\frac{\beta^2(b_{\mu\nu,R}b_{\nu\mu,R}+b_{\mu\nu,I}b_{\nu\mu,I})}{\overline{\omega}_{\mu,R}\,\overline{\omega}_{\nu,R}}-16\,\overline{\omega}_{\mu,I}\overline{\omega}_{\nu,I}\right]^{1/2} \tag{38}$$

$\mu\neq\nu$, $\mu,\nu=1,2,\ldots N_c$.

Case (C): Combination resonance of difference type

The boundaries of the regions of instability of difference type are given by

$$\left|\frac{\Omega}{2\omega_0}-\frac{1}{2}(\overline{\omega}_{\nu,R}-\overline{\omega}_{\mu,R})\right|<\frac{1}{8}\frac{(\overline{\omega}_{\mu,I}+\overline{\omega}_{\nu,I})}{(\overline{\omega}_{\mu,I}\,\overline{\omega}_{\nu,I})^{1/2}}\left[\frac{\beta^2(b_{\mu\nu,I}b_{\nu\mu,I}-b_{\mu\nu,R}b_{\nu\mu,R})}{\overline{\omega}_{\mu,R}\,\overline{\omega}_{\nu,R}}-16\,\overline{\omega}_{\mu,I}\overline{\omega}_{\nu,I}\right]^{1/2},\quad \nu>\mu,\mu,\nu=1,2,\ldots N_c. \tag{39}$$

3. RESULTS AND DISCUSSION

The geometrical and material properties of the sandwich beam used for the numerical analysis purpose is listed in the Table-1. The skins are assumed to be of aluminium. The geometrical parameters of the beam are same as those taken in reference,[9]. The electrorheological fluid with mass density of 1700kg/m^3 used in this study is same as that considered in reference, [9]. Based on the existing information on the ER material pre-yield rheology, only the electric field dependence of ER materials in the pre-yield regime has been considered. On the basis of the experimental data available, the complex modulus of the used ER fluid can be expressed as $G_2= G'+ G''i$, where the shear storage modulus $G'=C*E^2$, constant $C=50000$ and the loss modulus $G''=2600E+1700$, and E is the electric field in kV/mm. The same relation has been used for the Young's modulus.

Table-1, Dimensions and material properties of the sandwich beams

Young's modulus E_1, E_3	7x 10^{10}	Thickness t_2 (mm)	0.74
Density ρ_1, ρ_3 (kg/m^3)	2700	Thickness t_3 (mm)	0.74
Density ρ_2 (kg/m^3)	1700	Length (L) of the	381
Thickness t_1 (mm)	0.74	Width (b) of the beam	25.4

The validation of the present algorithm and calculations are first done by comparing the natural frequencies for the first five modes calculated from the present analysis with those obtained by Yalcintas and Coulter[9]. Complex shear modulus of the ER fluid has been taken as 612500*(1+0.011) N/m^2 for electric field strength 3.5 kV/mm. Comparison of numerical results shows a good agreement.

The variation of the fundamental buckling load parameter (P_b), defined as the ratio of fundamental buckling load to P^*, with core thickness parameter (t_2/t_1) is shown in figure-3

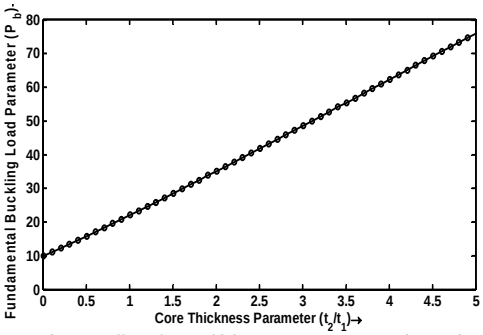

Figure -3,Effect of Core Thickness Parameter on Fundamental , Buckling Load Parameter Electric Field Strength, 3.5kV/mm, α=0.0.

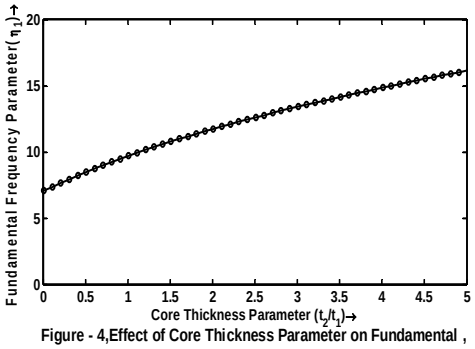

Figure - 4,Effect of Core Thickness Parameter on Fundamental , Frequency Parameter Electric Field Strength, 3.5 kV/mm, α=0.0.

It is seen from the figure that for fixed –free end condition of the beam the fundamental buckling load increases linearly with increase in t_2/t_1. Figure-4 shows the effect of core thickness parameter on fundamental frequency parameter (f). The fundamental frequency parameter is defined as the ratio of fundamental frequency of the sandwich beam to ω_o . The variation of fundamental frequency parameter with core thickness parameter shows the similar trend as those for fundamental buckling load. The variation of fundamental system loss factor (η) with core thickness parameter is shown in figure-5. For all the four boundary conditions the fundamental loss factor increases with increase in core thickness parameter. It is revealed from the figure that the rate of increase of fundamental loss factor with core thickness parameter is very high for low values (0.01 to 1.5) and for higher values of t_2/t_1 though the η increases the rate of increase is comparatively less.

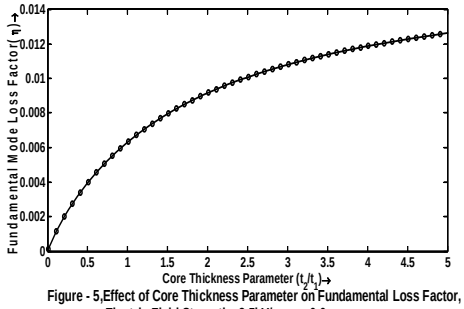

Figure - 5,Effect of Core Thickness Parameter on Fundamental Loss Factor, Electric Field Strength , 3.5kV/mm,α=0.0 .

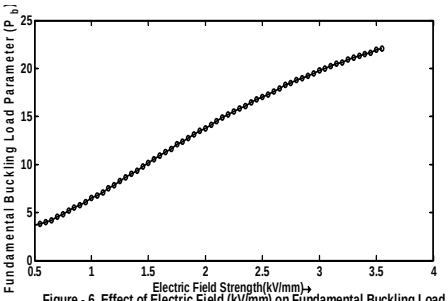

Figure - 6 ,Effect of Electric Field (kV/mm) on Fundamental Buckling Load Parameter t_2/t_1=1.0, α=0.0 .

In figure-6 the effect of electric field strength of (E) on fundamental buckling load parameter is shown. It can be observed that the fundamental buckling load increases with increase in electric field strength. Figure-7 shows the variation of fundamental frequency parameter with electric field strength. The behavior is same as those for fundamental buckling load.Figure-8 shows the instability regions for cases in which stiffness of the viscoelastic core of the beam has been calculated considering only shear deformation of the core and stiffness calculated considering the shear, longitudinal and transverse deformation of the core. It is seen that for the latter case the instability regions relocate themselves at lower frequencies. This means that there is reduction in stability of the beam. Hence for soft cored sandwich beam all the three flexibilities should be considered.

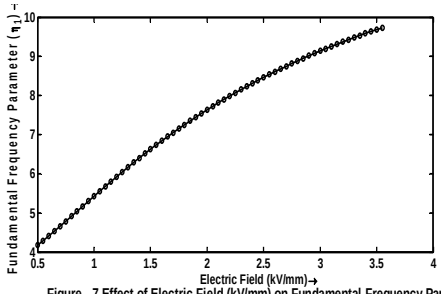

Figure - 7,Effect of Electric Field (kV/mm) on Fundamental Frequency Parameter, t_2/t_1=1.0 , α=0.0 .

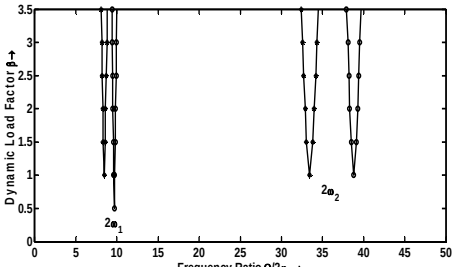

Figure - 8, Instability Regions: t_2/t_1 =1.0,E=3.5,Shear Strain only=0.0,o, Shear, Transverse & Longitudinal strain,*,

Figure-9 shows the effect of electric field strength on the first two instability regions of simple resonance. It is observed that with the increase in electric field strength, the instability regions shift to higher frequency of excitation and their areas also decrease. This means that the increase in electric field strength enhances the stability of the beam. Figure-10 shows the effect of core thickness parameter on the first two instability regions of simple resonance of the beam. It is seen that increase in core thickness parameter shifts the occurrence of instability regions to higher excitation frequency and their areas also decreases with increase in thickness ratio. So the increase in thickness ratio improves the stability behaviour of the beam.

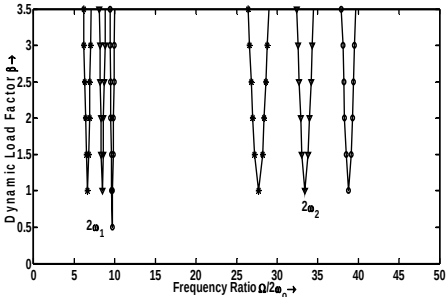

Figure - 9,Effect of Electrical Field Strength (E in kV/mm) on Instability Regions g =5.0, t_2/t_1 =1.0, α =0.0, E=3.5,O ,E=2.5,v , E=1.5,*, .

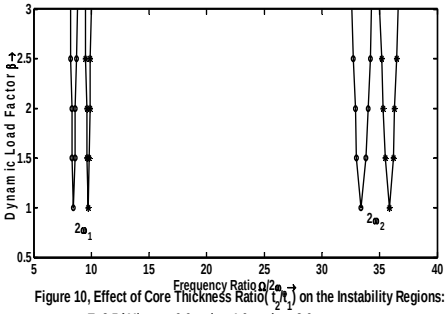

Figure 10, Effect of Core Thickness Ratio(t_2/t_1) on the Instability Regions: E=3.5 kV/mmα=0.0,, t_2/t_1 =1.0,o,t_2/t_1 = 2.0,*,

4. CONC LUSION

The present work investigates the dynamic stability of a sandwich beam with a soft electrorheological fluid core. For a cantilever beam the fundamental buckling load and the fundamental frequency increase with increase in thickness ratio for $5.0 \geq t_2/t_{12} \geq 0.01$ .The system fundamental loss factor increases with increase in thickness ratio for $5.0 \geq t_2/t_{12} \geq 0.01$. The fundamental buckling load and fundamental natural frequency increase with increase in electric field strength. The increase in electric field strength and core thickness has stabilizing effect.

REFERENCES

1. Winslow, W.M. Induced Fibration of Suspensions, Journal of Applied Physics, **20(12)**, 1137–1140, (1949).
2. Block, H. and Kelly, J.P. "Electro-rheology", J.Phys. D: Appl. Phys., **21**, 1661-1667, (1988).
3. Coulter, J.P. Engineering application of electrorheological materials, J Intell Mater Syst Struct, **4**,248–59, (1993).
4. Weiss, K.D., Coulter, J.P., and Carlson, J.D. Material aspects of electrorheological system, J Intell Mater Syst Struct,**4(1)**,13–34, (1993).
5. Gandhi, M.V., Thompson, B.S. and Choi, S.B. A New Generation of Innovative Ultra-advanced Intelligent Composite Materials Featuring Electro-rheological Fluids: An Experimental Investigation, Journal of Composite Materials, **23**, 1232–1255, (1989).
6. Carlson, J.D., Coulter, J.P., and Duclos, T.G. Electrorheological Fluid Composite Structures, US Patent No. 4, 23, 057, (1990).
7. Yalcintas, M. and Coulter, J.P. Analytical modeling of electrorheological material based adaptive beams, J Intell Mater Syst Struct, **6**,488–97, (1995).
8. Yalcintas, M. and Coulter, J.P. Electrorheological material based adaptive beams subjected to various boundary conditions, J Intell Mater Syst Struct ,**6**,700–17,(1995).
9. Don, D.L. and Coulter, J.P. An Analytical and Experimental Investigation of Electrorheological Material based Beam Structures, J Intellegent Material Systems and Structures, **6**, 6846-853, (1995).
10. Yalcintas, M. and Dai, H. Magnetorheological and Electrorheological Materials in Adaptive Structures and their Performance Comparison, Smart Materials and Structures,**8(5)**,560–573, (1999).
11. Lee, C.Y. Finite element formulation of a sandwich beam with embedded electro-rheological fluids, J Intell Mater Syst Struct, **6**,718–28(1995).
12. Rezaeepazhand,J. and Pahlavan,L. Transient Response of Sandwich Beams with Electrorheological Core , Journal of Intelligent Material Systems and Structures, first published on July 11, 2008 as doi:10.1177/1045389X08090313,(2008).
13. Brown, J.E., Hutt, J.M., and Salama, A.E. Finite element solution to dynamic stability of bars, AIAA J., **6**, 1423-1425, (1968).
14. Abbas, B.A.H. Dynamic stability of a rotating Timoshenko beam with a flexible root, Journal of sound and vibration, **108**, 25 – 32, (1986).
15. Abbas, B.A. H. and Thomas, J. Dynamic stability of Timoshenko beams resting on an elastic foundation, Journal of sound and vibration, **60**, 33 – 44, (1978).
16. Yokoyama, T. Parametric instability of Timoshenko beams resting on an elastic foundation, Computer and structures, **28**, 207 – 216, (1988).
17. Briseghella,G., Majorana,C.E., and Pellegrino,C., Dynamic stability of elastic structures: a finite element approach, Computer and structures, **69**,11-25,(1998).
18. Svensson, I. Dynamic instability regions in a damped system, Journal of Sound and Vibration, **244**, 779-793, (2001).
19. Mohanty, S.C. Dynamic Stability of Beams Under Parametric Excitation, Ph.D. thesis, N.I.T,Rourkela, Orissa, India, 73-104, (2005).
20. Yeh, J.Y., Chen, L.W. and Wang, C.C. Dynamic Stability of a Sandwich Beam with a Constrained Layer and Electrorheological fluid Core, Journal of Composite Structures, **64**,47–54, (2004).
21. Mohanty, S.C. Parametric Instability of a Pretwisted Cantilever Beam with Localised Damage, International Jr. of Acoustics and Vibration, **12(4)**,153-161,(2007).
22. Saito, H. and Otomi, K. Parametric response of viscoelastically supported beams, Journal of Sound and Vibration, **63**, 169 – 178, (1979).